Capacity configuration optimisation of hybrid renewable energy system using improved grey wolf optimiser

Huili Wei and Shan Chen

School of Electrical and Information Engineering,
Jiangsu University,
Zhenjiang, Jiangsu, China
Email: 854666792@qq.com
Email: schen@ujs.edu.cn

Tianhong Pan*, Jun Tao and Mingxing Zhu

School of Electrical Engineering and Automation,
Anhui University,
Hefei, Anhui, China,
Email: thpan@ahu.edu.cn
Email: Jun.Tao@ahu.edu.cn
Email: xysah@163.com
*Corresponding author

Abstract: An appropriate capacity configuration of the Hybrid Renewable Energy System (HRES) contributes to reduce the equipment cost of the system configuration, and improve the operational reliability of the system. Aiming at minimising the Annualised Cost of System (ACS) and the Loss of Power Supply Probability (LPSP), a capacity configuration optimisation model of a PV-wind HRES is set up in this work. An improved Grey Wolf Optimiser (iGWO) is proposed to optimise the system's configuration. First, the Tent chaotic strategy is used to initialise the population. Then, the convergence factor is improved to balance the local and global search ability of GWO. Finally, the meteorological data of the wind speed and solar radiation in a typical year in Zhenjiang, China, are taken as a case to verify the economy and feasibility of the optimal configuration. The results show that the proposed method not only ensures the operation reliability, but also improves the economic performance of HRES.

Keywords: hybrid renewable energy system; optimisation; capacity configuration; improved grey wolf optimiser.

Reference to this paper should be made as follows: Wei, H., Chen, S., Pan, T., Tao, J. and Zhu, M. (2022) 'Capacity configuration optimisation of hybrid renewable energy system using improved grey wolf optimiser', *Int. J. Computer Applications in Technology*, Vol. 68, No. 1, pp.1–11.

Biographical notes: Huili Wei is a graduate student in Jiangsu University at China. Her research interests include energy management and control strategy of the PV-wind micro-grid.

Shan Chen is an Associate Professor in the School of Electrical and Information Engineering, Jiangsu University, Zhenjiang, China. Her research interests include electrotechnics and electronics, modelling for non-linear system and run-to-run control.

Tianhong Pan is a Professor in the School of Electrical Engineering and Automation, Anhui University. He received his PhD degree in Control Theory and Control Engineering from Shanghai Jiao Tong University, Shanghai, China in 2007. His research interests include multiple model approach and its application, machine learning, virtual metrology, predictive control and run-to-run control theory and practice, etc.

Jun Tao is a Professor in the School of Electrical Engineering and Automation, Anhui University. His research interests include power and electron technology, power quality assessment, power system automation, etc.

Mingxing Zhu is a Professor in the School of Electrical Engineering and Automation, Anhui University. His research interests include power and electron technology, power quality assessment, etc.

1 Introduction

Owing the seasonal and periodical variations, neither a single wind energy nor a solar energy power system can provide the energy supply continuously and steadily.

Fortunately, making full use of the time complementary nature of the two resources can almost overcome the uncertainty and variability of the energies. The PV-wind HRES has higher energy efficiency and lower costs for the same electricity production (Saba et al., 2017). However, it is a challenging issue to analyse the performance of PV-wind HRES which combines the wind and solar generation systems together.

The standalone HRES supplies the load relying on power source in the system, and does not require the support of the power grid. To maintain the energy balance, it is necessary to configure each power capacity matching with wind and solar resource as well as load demand. When the system capacity is too large, the power demand can be satisfied. But it will cause the energy waste undoubtedly, and significantly affect the long-term economic performance. On the contrary, it is difficult to feed the load demand and even the power failure occurs if the system capacity size is too small, and directly leads to the decline of the system power supply reliability (Bhandari et al., 2015; Sultan et al., 2020). Therefore, rationally configure the capacity of HRES is conducive to saving the investment cost. Furthermore, the risk of additional loss due to power shortage is reduced, so the safety and reliability of the system are significantly improved.

To maintain the HRES working at optimal conditions in term of system investment cost and power supply reliability, many researches mainly focused on configuring the capacity of the HRES.

Zhang et al. (2019a) investigated the operational reliability of the hybrid solar-wind-battery power generation system, and put forward a non-dominated sorting genetic algorithm to optimise the system configuration. Sharafi and Elmekkawy (2014) considered the loss of load probability and loss of energy probability of the HRES, put forward a particle swarm optimisation and ε-constraint for the optimal system size, and achieved the long-term reliable operation of the HRES. Barakat et al. (2020) proposed the simulated annealing algorithm to optimise the LPSP, cost of energy and renewable energy fraction, and the optimal configuration from the aspects of system economic efficiency, energy efficiency, carbon emissions was presented. Yahiaoui et al. (2017) used a grey wolf optimiser to analyse the capacity allocation of HRES, with the optimisation goals of minimum ACS, which optimised the economic behaviour of the system.

In this work, GWO was introduced to configure the capacity of the HRES. The GWO is a swarm intelligent algorithm proposed by Mirjalili et al. (2014). The main inspiration of GWO is to imitate the hunting process of grey wolves to deal with optimisation problems. Compared with other swarm intelligent algorithms, the GWO has the advantages of high accuracy, fewer control parameters, and fast convergence speed. It is easy to implement and widely used in parameter optimisation, workshop scheduling, path planning and economic load dispatching (Sulaiman et al., 2015; Kamboj et al., 2016), etc.

In addition, to increase the efficiency of GWO, two improvement strategies are proposed in this work. First, the chaotic algorithm is used to initialise the population. Then, a self-adaptive convergence factor is introduced to balance the global and the local search ability of GWO. Two performance indicators (i.e., ACS and LPSP) are used to establish the configuration optimisation model of the HRES, and the real-time meteorological data of Zhenjiang area are taken as an example to verify the rationality of the proposed scheme.

Organisation of the remaining paper is as follows. The mathematical models of the HRES are described in Section 2. The objective functions and constraints of the configuration optimisation are implemented in Section 3. The optimisation algorithm description and improvement strategies are given in Section 4. The case analysis of the iGWO is presented in Section 5. The conclusion is drawn in Section 6.

2 Model of hybrid system components

In this study, the HRES includes five components comprising a wind turbine, PV panel, controller, battery pack and load (shown in Figure 1).

The wind turbine and PV panels convert the wind and solar resources into the electrical energy. The controller is mainly responsible for AC/DC conversion of the generated electrical energy. The battery pack exists as a backup system. It is used for energy storage, power supply and voltage stabilisation.

2.1 PV system model

The output of the PV system is determined by the solar radiation, the ambient temperature, the irradiation area, and the conversion efficiency of PV panel. Considering the practice engineering, the PV system is modelled based on the available solar radiation at installation site. The output of the PV system is given as follows (Wang et al., 2017).

$$P_{PV} = P_{STC} G_{AC} \frac{1+\tau\left(t_c - t_r\right)}{G_{STC}} \tag{1}$$

where P_{PV} is the stable output power of the PV panel, P_{STC} the maximum test power under standard test conditions (i.e., the solar irradiance is 1000 W/m^2, and the ambient temperature is 25ºC), G_{AC} the current solar irradiance, G_{STC} the solar irradiance under standard test conditions of $1000\,W/m^2$, τ the power temperature coefficient, –0.0043ºC, t_c the operating temperature of PV panel and t_r the reference ambient temperature of 25ºC.

Figure 1 Block diagram of the HRES

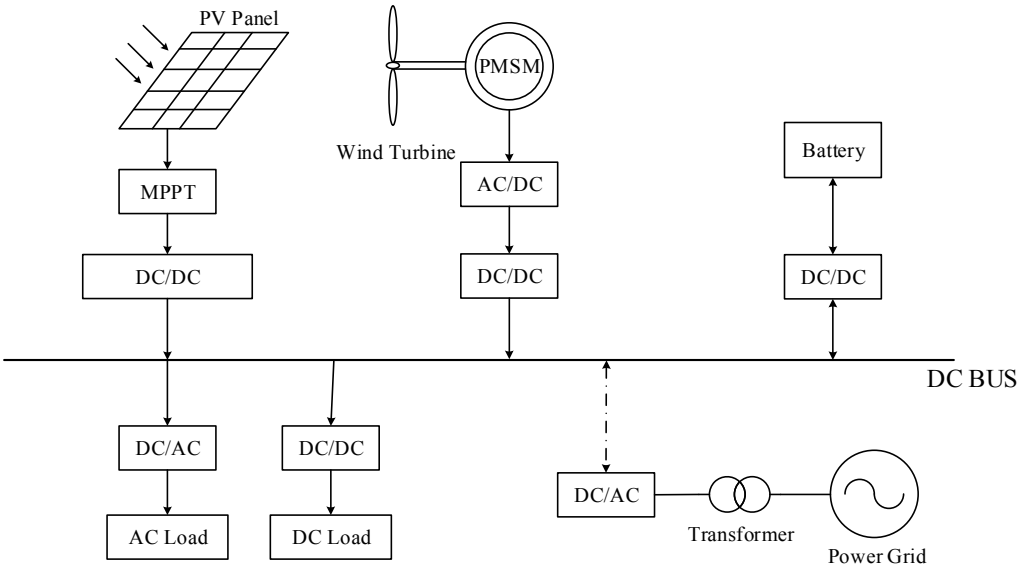

2.2 Wind turbine system model

There are three factors affecting the real-time output of the wind turbine, i.e., the wind speed distribution, the output characteristics of the wind turbine and the tower height. Wind speed changes with height, and the wind speed data obtained from meteorological department is usually the wind speed at the anemometer. Wind speed at the rotation axis of the wind turbine can be calculated by equation (2) (Baghaee et al., 2017).

$$v(t) = v_{ref}(t) \cdot \left(\frac{H_{WT}}{H_{ref}} \right)^{\sigma} \tag{2}$$

where $v(t)$ is the real-time wind speed at the rotating axis of the wind turbine, $v_{ref}(t)$ the wind speed measured by the anemometer, H_{WT} the tower height, H_{ref} the installation height of the anemometer, σ the exponent law coefficient, generally taken as 1/7–1/4.

In fact, the power curve of a typical wind turbine is nonlinear. The wind turbine is unable to start if the wind speed is lower than the cut-in speed v_i. The power output increases parabolically as the wind speed increases from the cut-in wind speed v_i to the rated wind speed v_r. The rated power P_r is produced when the wind speed is greater than the rated wind speed v_r but lower than the cut-out wind speed v_o. If the wind speed exceeds the cut-out wind speed v_o, the wind turbine will be shut down for safety considerations. The wind turbine output characteristic is expressed as follows (Eryilmaz et al., 2021).

$$P_{WT} = \begin{cases} 0 & (v < v_i, v > v_o) \\ P_r \cdot \dfrac{v - v_i}{v_r - v_i} & (v_i < v < v_r) \\ P_r & (v_r < v < v_o) \end{cases} \tag{3}$$

Based on the mathematical model, the approximate power characteristic curve of the wind turbine is shown in Figure 2.

2.3 Battery model

For a further understanding of the real the remaining capacity of a battery, it is necessary to know the State of Charge (SOC). The SOC of a battery at t moment is determined by the charged state at $t-1$ moment, the charge and discharge capacity from $t-1$ moment to t moment and the self-discharge rate (Das et al., 2019).

When the battery is charged, the SOC at t moment is as follows:

$$SOC(t) = (1-\eta)SOC(t-1) + \frac{P_{ch}(t)\eta_{ch}\Delta t}{E_r} \tag{4}$$

Figure 2 Output-power feature of wind turbine

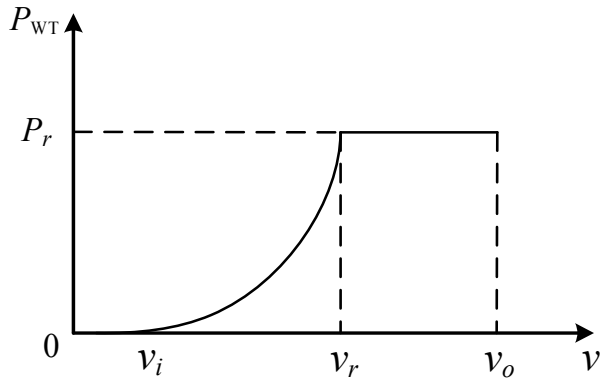

When the battery is discharged, the SOC at t moment is as follows:

$$SOC(t) = (1-\eta)SOC(t-1) - \frac{P_{dis}(t)\Delta t}{\eta_{dis}E_r} \tag{5}$$

where η, η_{ch}, η_{dis}, $P_{ch}(t)$, $P_{dis}(t)$ and E_r are the battery self-discharge rate, charge efficiency, discharge efficiency, charge power, discharge power and rated capacity, respectively; Δt is the sampling step and set to 1 in this study.

3 Optimisation model of HRES

Compared with the single power supply system, a HRES needs to consider more decision variables and parameters, and the optimisation goals and the constraints can be described as follows:

3.1 Objective functions of optimisation model

3.1.1 ACS economic model concept

The ACS is considered to the best benchmark of economic analysis of the HRES, which is composed of the annual capital cost, annual operation and maintenance cost, and annual replacement cost. The ACS evaluates the total cost of the entire life cycle of the HRES. It not only takes the account into the initial cost of the project, but also comprehensively considers the additional cost in the later period after the HRES operation. Therefore, the ACS is an important indicator to evaluate the long-term economic performance of the HRES. It can be described mathematically below (Salisu et al., 2019; Akram et al., 2020; Javed et al., 2019).

1) *The annual capital cost*:

$$C_o = f_{cr} \sum_{i=1}^{3} N_i p_i \tag{6}$$

where i is the different types of generating components (i.e., the wind turbine, PV panel and battery); N_i and p_i are the number and price of each power source, respectively; f_{cr} is the capital recovery factor, a portion that the amount of recoverable cash flow at a specified interest rate each year. The calculation expression of the capital recovery factor is expressed as follows:

$$f_{cr} = \frac{r(1+r)^{y_{rep}}}{(1+r)^{y_{rep}} - 1} \tag{7}$$

where y_{rep} is the lifetime of the power components, and r the annual real interest rate, which is expressed as follows:

$$r = \frac{r' - f}{1+f} \tag{8}$$

where r' is the nominal interest rate, 8.25% and f the annual inflation rate, 8.17%.

2) *The maintenance cost of the system*: The maintenance cost of each power generation component during the system lifetime is expressed as follows:

$$C_m = y_{rep} \sum_{t=1}^{8760} \sum_{i=1}^{3} \varepsilon_i N_i P_i(t) \Delta t \tag{9}$$

where t is a certain sampling moment, N_i the number of different power generation units; $P_i(t)$ is the operating power of each power source at t moment; ε_i is the maintenance cost coefficient, which is defined as the required maintenance cost for per kilowatt-hour of electricity produced by the generating unit.

3) *The annual replacement cost*: The annual replacement cost is as follows (assuming only batteries need to be replaced).

$$C_r = C_{rep} \cdot SFF\left(r, y_{rep}\right) \tag{10}$$

where C_{rep} is the replacement cost of the battery, and y_{rep} the lifetime of battery pack in year. SFF, the sinking fund factor, is defined as the ratio to calculate the future value of a series of equal annual cash flows. It converts the replacement cost to the average annualised replacement cost over the lifetime of the components, and can be described as follows:

$$SFF = \frac{r}{(1+r)^{y_{rep}} - 1} \tag{11}$$

3.1.2 Loss of power supply probability

Since the intermittent solar radiation and the wind speed characteristics greatly affect the electricity production, the power reliability analysis is considered a significant step in any system optimisation. The optimal configuration of a HRES is to find a best compromise between the ACS and system reliability.

A reliable power system means a system has enough power to feed the load demand during a certain period. The concept of LPSP is introduced in this study. LPSP is defined as the probability that the HRES fails to satisfy the load demand during a given period (Yang et al., 2009). The parameter characterises that the HRES cannot meet the load demand due to the insufficient electricity production of wind turbine and PV panel, which can be considered as a representation of the power supply reliability of HRES. LPSP ranges from 0 to 1, where 0 means that the output of the HRES can always provide enough power to meet the load demand, and 1 indicates that the load cannot be satisfied throughout the lifetime. Therefore, the value of LPSP should be small enough. The equation for the LPSP is as follows:

$$LPSP = \frac{\sum_{t=1}^{m} \left[P_L(t) - \sum_{i=1}^{3} P_i(t) \right]}{\sum_{t=1}^{8760} P_L(t)} \tag{12}$$

where m is the number of hours that unable to meet the load power requirements within a given time. The numerator indicates the electricity shortage of the HRES, and the denominator indicates the total electric energy demand within a given time.

3.2 Constraints of optimisation model

1) *Power source quantity constraint*: Considering the limitation of construction land, the total floor space of the HRES is S, the length L, the width B, and the constraints of the number of each generation unit is as follows (Liao et al., 2019).

$$\begin{cases} 0 \le N_{WT} \le \left[\dfrac{L}{8d}+1\right]\left[\dfrac{B}{4d}+1\right] \\ 0 \le N_{PV} \le \left[\dfrac{S}{S_{PV}}\right]\alpha_{PV} \\ 0 \le N_{BAT} \le \left[\dfrac{S}{S_{BAT}}\right] \end{cases} \tag{13}$$

where $[x]$ is the integer part of x, N_{WT}, N_{PV}, and N_{BAT} are the number of the wind turbine, the PV panel and the battery pack, respectively; d is the diameter of the wind rotor, S_{PV} the area of a single PV panel α_{PV} the shading coefficient, S_{BAT} the area of a single battery pack.

2) *Energy balance constraint*: The generated electrical power of the PV-wind HRES should be greater than or equal to the estimated maximum load power demand P_L (Zhang et al. 2019b).

$$\sum P_{PV} + \sum P_{WT} \ge P_L \tag{14}$$

3) *Battery storage limits constraint*: To avoid overcharge and improve the battery lifetime, it is necessary to restrict the charging and discharging process of the battery. The energy constraint of battery is expressed as equation (15) (Moradi et al., 2018).

$$SOC_{\min} \le SOC \le SOC_{\min} \tag{15}$$

where $SOC_{\min}$ and $SOC_{\max}$ are the lower and upper limits of SOC of the battery, respectively.

The battery charge and discharge power constraints are expressed as follows (Abbes et al., 2014).

$$\begin{cases} 0 \le P_{ch}(t) \le \\ \min\left\{P_{ch\_\max}, \dfrac{E_r\left(SOC_{\max}-(1-\eta)SOC(t-1)\right)}{\eta_c \Delta t}\right\} \\ 0 \le P_{dis}(t) \le \\ \min\left\{P_{dis\_\max}, \dfrac{E_r\left((1-\eta)SOC(t-1)-SOC_{\min}\right)\eta_d}{\Delta t}\right\} \end{cases} \tag{16}$$

where $P_{ch\_\max}$ and $P_{dis\_\max}$ are the maximum allowable power for continuous charge and discharge of the battery, respectively.

Based on the above analysis, the objective functions and constraints of the PV-wind HRES are summarised as follows:

$$\begin{cases} \min \quad ACS = C_o + C_m + C_r \\ \min \quad LPSP \\ s.t. \quad \text{equation (13)} - \text{equation (16)} \end{cases} \tag{17}$$

As can be seen that the configuration programming of the HRES belongs to a multi-objective optimisation problem, that is formed with three decision variables, two objective functions and four constraints with functional relationships.

4 System optimisation using grey wolf optimiser

In recent researches, the GWO has been applied for multi-objective optimisation especially for dynamically searching for the optimal configuration (El-Fergany and Hasanien, 2015; Gupta and Deep, 2020). An iGWO is proposed to optimise the configuration of the PV-wind HRES in this paper. The number of the wind turbine N_{PV}, PV panel N_{PV} and battery N_{BAT} are selected as the decision variables of multi-objective optimisation. Under the limitation of the above-mentioned constraints, the optimal configuration of each power component (i.e., the wind turbine, PV panel and battery) is obtained, thereby minimising the value of objective functions.

4.1 GWO description

The grey wolves are gregarious animals of the canine family, usually consisting of 5–30 wolves in a group. Grey wolves hunt in a strict social hierarchy, naming alpha (α) wolf, beta (β) wolf, delta (δ) wolf and omega (ω) wolf from the top to the bottom (Mirjalili et al., 2016), as shown in Figure 3.

Figure 3 Hierarchy of grey wolves (dominance decreases from top down)

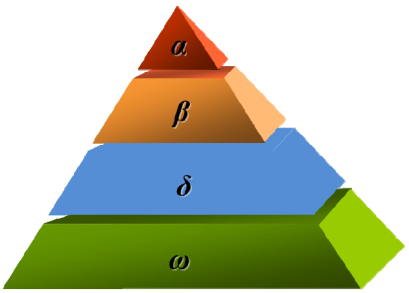

The α wolf, as the leader of the wolf pack, is the individual with the strongest management ability in the wolf pack, and always makes decisions about hunting process in the search for global optimum. The β wolf and δ wolf are the two individuals with the second and the third fitness function value, respectively. They are the candidates for the α wolf, and assist the α wolf to manage the wolf pack during hunting. The ω wolves are the lowest dominated hierarchy. They follow three wolves in search of the prey, which play an important role in the stability of the wolf pack order.

In GWO, the whole hunting process of the wolves consists of three behaviours: encirclement, pursuit and attack (Komaki and Kayvanfar, 2015), and finally the prey is captured (that is, the global optimal solution is obtained). The mathematical model of hunting process of GWO is described as follows:

1) *Encircling prey*: The grey wolves encircle the prey after recognising its location. In this process, the following equations are proposed to simulate the encircling behaviour of the grey wolves.

$$\vec{D} = \left| \vec{C} \cdot \vec{X}_p(k) - \vec{X}(k) \right| \tag{18}$$

$$\vec{X}(k+1) = \vec{X}_p(k) - \vec{A} \cdot \vec{D} \tag{19}$$

where D is the distance between the grey wolf and the prey, k the current iteration, $\vec{X}_p(k)$ the position of the prey (i.e., the optimal solution) after k iterations, $\vec{X}(k)$ the position of the grey wolf (i.e., the potential solution) after k iterations; $\vec{A}$ and $\vec{C}$ are the coefficient vectors, and can be calculated as follows:

$$\vec{A} = 2\vec{a} \cdot \vec{r}_1 - \vec{a} \tag{20}$$

$$\vec{C} = 2 \cdot \vec{r}_2 \tag{21}$$

where $\vec{r}_1$ and $\vec{r}_2$ are the random vectors between 0 and 1; $\vec{a}$ is the convergence factor, which decreases linearly from 2 to 0 during the process of the iterations.

$\vec{A}$ is the weight coefficient of the distance among α, β, δ wolf and ω wolf. It determines the location updating of the grey wolf individual. $\vec{C}$ is the weight coefficient of search distance that ω wolf around α, β and δ wolf. It specifies the difficulty of the leadership wolves in the search process. By adjusting the values of $\vec{A}$ and $\vec{C}$, the wolves can reach any position in the search area.

2) *Pursuing prey*: After encircling the prey, the β and δ wolves hunt the prey in the leadership of the α wolf. The position update mechanism of the grey wolves and prey in the pursuing process is shown in Figure 4 (a), and the update equations are as follows:

$$\begin{cases} \vec{D}_\alpha = \left| \vec{C}_1 \cdot \vec{X}_\alpha - \vec{X} \right| \\ \vec{D}_\beta = \left| \vec{C}_2 \cdot \vec{X}_\beta - \vec{X} \right| \\ \vec{D}_\delta = \left| \vec{C}_3 \cdot \vec{X}_\delta - \vec{X} \right| \end{cases} \tag{22}$$

$$\begin{cases} \vec{X}_1 = \vec{X}_\alpha - \vec{A}_1 \cdot \vec{D}_\alpha \\ \vec{X}_2 = \vec{X}_\beta - \vec{A}_2 \cdot \vec{D}_\beta \\ \vec{X}_3 = \vec{X}_\delta - \vec{A}_3 \cdot \vec{D}_\delta \end{cases} \tag{23}$$

$$\vec{X}_p(k+1) = \frac{\vec{X}_1 + \vec{X}_2 + \vec{X}_3}{3} \tag{24}$$

where $\vec{D}_\alpha$, $\vec{D}_\beta$, $\vec{D}_\delta$ indicate the distance between α wolf, β wolf, δ wolf and ω wolf, respectively.

3) *Attacking prey*: Attacking is the final step in the hunting process. In this process, the grey wolves disperse away from the prey when $\left|\vec{A}\right| > 1$, corresponding to the global search. On the contrary, when $\left|\vec{A}\right| < 1$, the grey wolf group shrink the encirclement to final attack and capture the prey (i.e., the optimal solution), corresponding to the local search (Dhargupta et al., 2020), as shown in Figure 4(b).

4.2 Convergence factor nonlinear adjustment strategy

If the global and local search are not well coordinated, the probability of the GWO falling into a local optimum increase, thereby deteriorating its convergence performance (Liu et al., 2019).

Based on equation (20), $\vec{r}$ varies randomly between 0 and 1, so the convergence factor $\vec{a}$ decreases linearly from 2 to 0, which will cause the fluctuation of the coefficient vector $\vec{A}$ with the iterations increasing. In other words, $\vec{a}$ determines the values of $\vec{A}$ and $\vec{A}$ is a random vector in the interval $[-a, a]$. Therefore, the variation of $\vec{a}$ influence the greatly influence the global and local search capabilities of the GWO. However, $\vec{a}$ changes linearly during the search process in the standard GWO, and the linearly decreasing strategy of the convergence factor cannot fully reflect the actual search process. To ensure the balance between the global search diversity and local search accuracy, and overcome the defect that the decreased searching ability of grey wolf during the later stage of iteration, a non-linear change convergence factor update strategy is proposed in this study. Its mathematical expression is shown in equation (25).

$$\vec{a} = 2 - 2\left(\frac{1}{e-1} \times (e^{\frac{k}{k_{\max}}} - 1) \right) \tag{25}$$

where k is the current iterations, and $k_{\max}$ the maximum number of iterations.

Based on the equation (25), the value of $\vec{a}$ decreases as the number of iterations increases. At the early period of the iteration, the value of $\vec{a}$ is large, so the grey wolves enlarge the search scopes, which is conducive to predict the general direction of the prey. In the last stage of iteration, the value of $\vec{a}$ is small, so the grey wolf shorter the searching step, which is beneficial to accurately locate the global optimal solution. The variation in the non-linear convergence factor $\vec{a}$ with respect to the number of iterations is shown in Figure 5.

4.3 Population initialisation based on Tent chaotic

To improve the uniformity and diversity of the initial population distribution, chaos is introduced in GWO in this

study (Jitkongchuen et al., 2015). In general terms, chaos is a kind of random motion that appears in nonlinear dynamic system. It is often manifested as the simple law behind random phenomena, which is non-periodic, non-convergent, ergodic and regularity (Pecora and Carroll, 1990).

Figure 4 Position updating mechanism and the effect of $\vec{A}$ in GWO. (a) Position updating mechanism (b) 2D position vectors and effect of $\vec{A}$

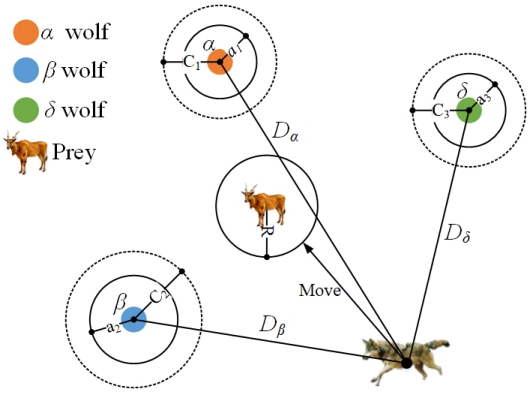

(a)

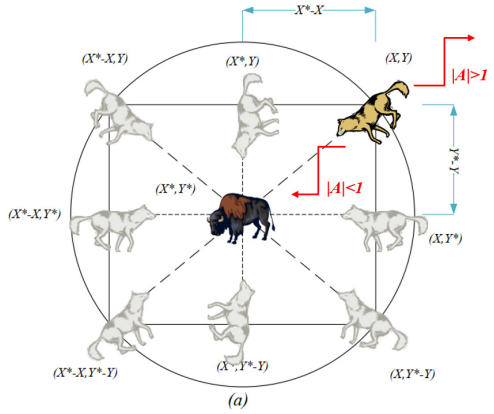

(b)

Figure 5 Variation of convergence factor with respect to number of iterations

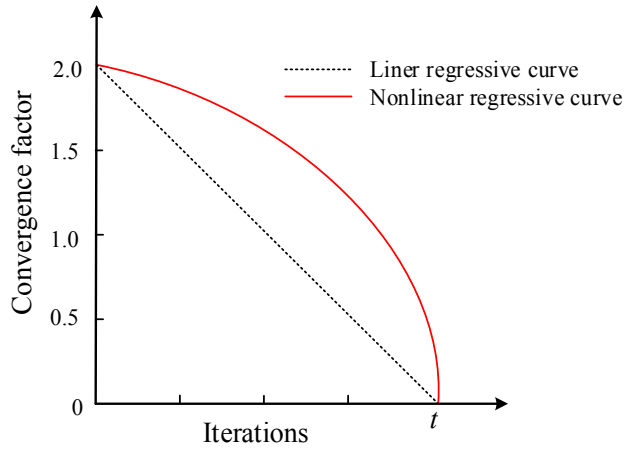

The Logistic map is widely introduced to generate chaotic sequences in the optimisation. However, the uniformity of the chaos system generated by Logistic mapping between 0 and 1 is poor, and its probability density function presents a Chebyshev-type distribution with dense at both ends and sparse in the middle. Plenty of research have been carried out to identify that Tent chaotic map shows better ergodicity and uniformity than Logistic map, and the chaotic optimisation method based on Tent map has higher searching efficiency (Gandomi and Yang, 2014; Chen et al., 2020).

Therefore, the Tent chaotic sequence is employed to improve the GWO. The improvement mechanism is as follows: when the GWO get struck at local optimal solution, the tent chaotic map is introduced to change the updating strategy of position of grey wolf individual and guides the population to perform a certain number of chaotic updating. As a result, the search process is out of the local optimum, and the global optimisation ability of the GWO is improved.

The mathematical expression of the Tent map is as follows (Yang et al., 2007).

$$x_{k+1} = \begin{cases} 2x_k & 0 \le x_k \le \dfrac{1}{2} \\ 2(1-x_k) & \dfrac{1}{2} < x_k \le 1 \end{cases} \tag{26}$$

After the Bernoulli transformation, the displacement transformation can be expressed by:

$$x_{k+1} = 2(x_k) \bmod 1 \tag{27}$$

where x_k , x_{k+1} are the position of the grey wolf in the initial period after k and $k+1$ iterations, respectively; mod is the remainder operation symbol.

The configuration optimisation procedure of the PV-wind HRES based on iGWO is illustrated in Figure 6.

5 Case study

In this study, the researched HRES located in Zhenjiang city, China. Combined with the hourly meteorological data, the load demand profile, and the specification of each components, the optimal combination of the wind turbine, the PV panel and the battery of the HRES are determined.

The cut-in wind speed, rated wind speed, and cut-out wind speed of the wind turbine are 3 m/s, 10 m/s, 20 m/s, respectively. A GFM100-12 lead-acid battery pack was used to store energy. Based on the specification provided by battery maker, the rated capacity of a single battery pack is 100 Ah, and the efficiency of the battery is 0.8. The battery stops charging when the remaining capacity is greater than 90%, and the battery stop discharging when the remaining capacity is less than 10%. Therefore, the $SOC_{\min}$ and $SOC_{\max}$ of battery pack were set 0.1 and 0.9, respectively in this work. The specification of each power source is illustrated in Table 1.

Figure 6 Flow chart of capacity optimisation of PV-wind HRES

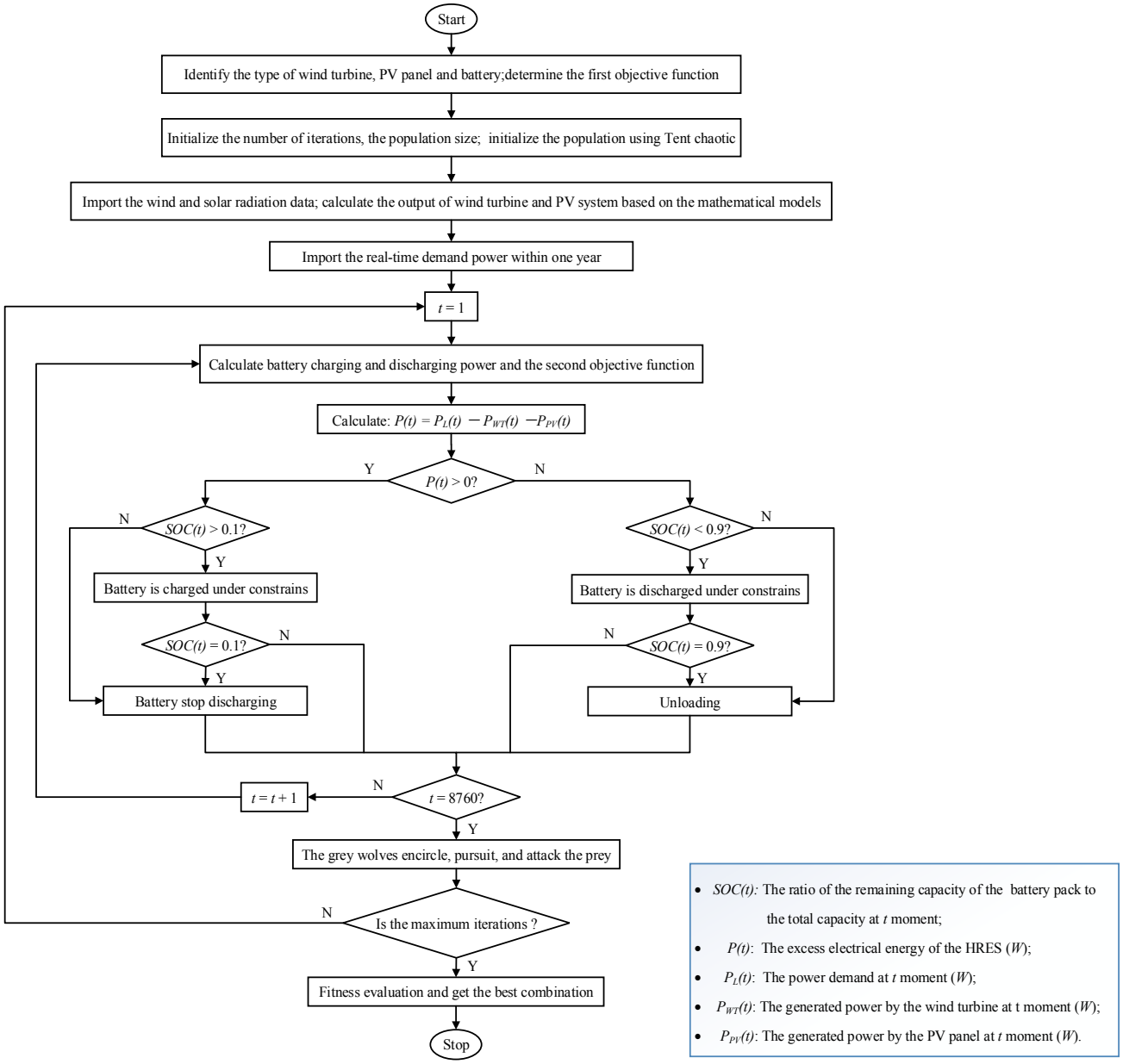

Table 1 Specification of each power sources

Power source	*Wind turbine*	*PV panel*	*Battery*
Power/Capacity	300 W	200 W	100 AH
Size	*R*=1.2 m	1200*650*30 mm	407*173*210 mm
Capital cost/ ($)	1500	850	500
Maintenance cost factor /($·(kW·h)$^{-1}$)	0.0187	0.0079	0.008
Lifetime/(year)	15	15	5

The hourly wind speed data profile, and the hourly solar radiation data profile are shown in Figures 7(a) and 7(b), respectively. The hourly environmental temperature profile, and the hourly load profile in Zhenjiang city are shown Figures 8(a) and 8(b), respectively.

Since the multi-objective functions are provided in this work, the Pareto front is introduced to clearly show the optimisation results. And the GWO and iGWO had been implemented with 30 search agents and 200 iterations.

The Pareto set of the standard GWO and the iGWO are illustrated in Figure 9. The optimal number of the components by the two algorithms are shown in Table 2.

Figure 7 Hourly wind speed and solar radiation profile of one year. (a) Hourly wind speed (b) Hourly solar radiation

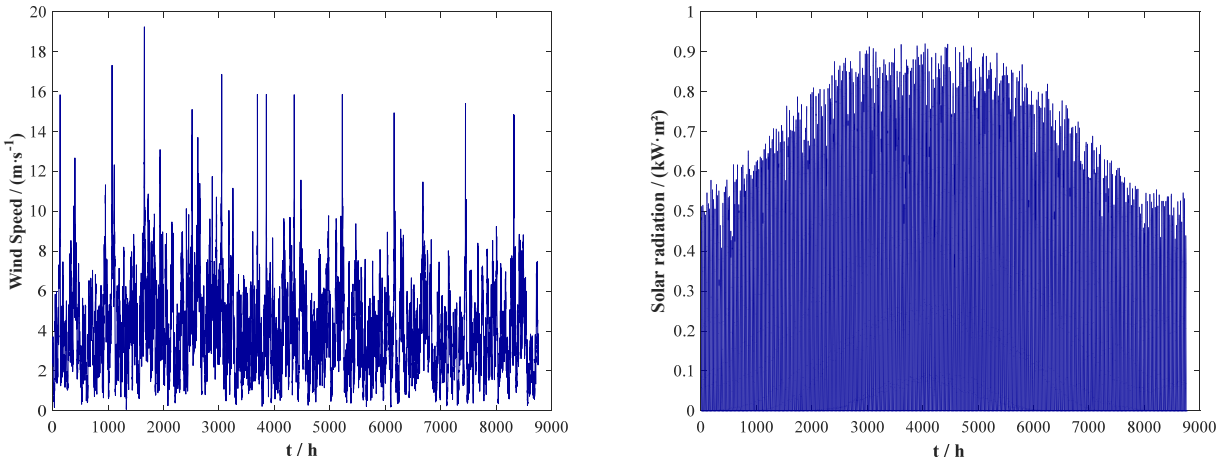

(a) (b)

Figure 8 Hourly temperature and load demand of one year. (a) Hourly temperature (b) Hourly load demand

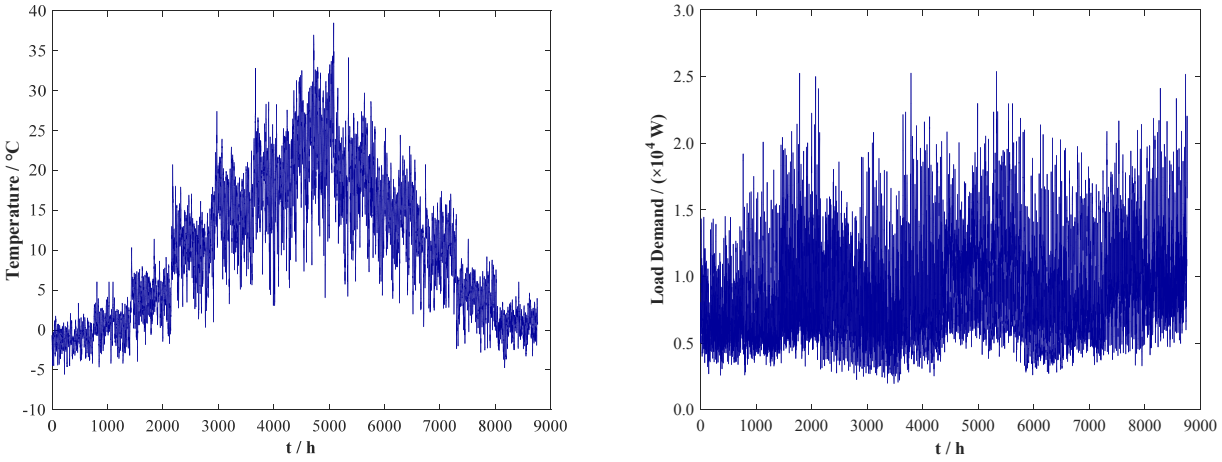

(a) (b)

Figure 9 Pareto set of the optimisation algorithms. (a) Pareto set of GWO (b) Pareto set of iGWO

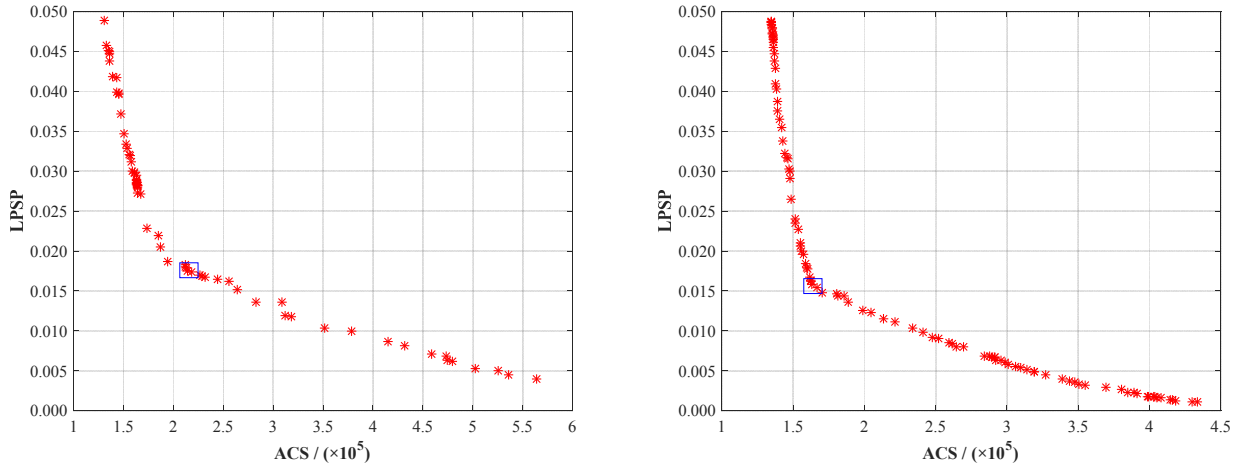

(a) (b)

Table 2 Capacity optimisation results

Optimisation algorithm	*PV panel*	*Wind turbine*	*Battery*	*ACS ($)*
Standard GWO	103	35	140	210,050
Improve GWO	79	24	110	158,150

It can be seen from the Figure 9 that the Pareto set of the iGWO was more uniform compare with the conventional GWO. According to Table 2, the iGWO for the optimal configuration at low cost was superior to that of the standard GWO.

As shown in Table 2, the simulation results showed that the optimal allocation of the HRES comprising 79 PV panels, 24 wind turbines, and 110 batteries. The number of photovoltaic cells was relatively large with two algorithms owing to the rich solar resource in Zhenjiang city. The capital cost of the system based on iGWO was 158150 $. The comparison showed that the iGWO contributed nearly by a 25% cost saving with respect to the simulation results based on the conventional GWO (210050 $). In optimisation results, the SOC of the battery was 0.0397, and the LPSP of the HRES was calculated as 0.016, indicating that the power system fully met the constraints and the load requirement.

6 Results and conclusion

The power supply reliability and annualised system cost are two major issues in the design of PV-wind HRES. To utilise wind and solar resources economically and efficiently, a multi-objective GWO algorithm based on Tent chaotic and improved convergence factor for the optimal configuration of HRES had been presented in this paper. Compared with conventional optimisation methods, the model aimed at system economic performance and reliability. It can be used to calculate the optimal system configuration, which realised the desired loss of power supply probability with the minimum annualised system cost. The main objectives of the optimisation problem were to minimise the total annual cost system and to determine the optimal configuration of the number PV panel, wind turbine and battery.

The introduced optimisation method had been applied to analyse a HRES in Zhenjiang city. The results showed that the presented iGWO achieved the optimum capacity allocation of the HRES with a relatively simple computational complexity and fast convergence rate. Consequently, the utilise of iGWO effectively improves the reliability and economy of the power supply system, which is of great significant merits to the research on the optimal configuration design of the PV-wind HRES.

In future work, there are some issues needed to be considered.

1) Sensitivity analysis should be performed to validate the impact of each components on the cost and reliability of the generation system.
2) New measures should be conducted to improve the efficiency of the algorithm.
3) Control strategies for the HRES under different types of uncertain practical environments should be researched.

Acknowledgements

This work is supported by Science and Technology Project of China Southern Power Grid (090000KK52190169/ SZKJXM2019669) and Key R&D Program of Jiangsu Province, China (Grant No. BE2018370).

References

Abbes, D., Martinez, A. and Champenois, G. (2014) 'Life cycle cost, embodied energy and loss of power supply probability for the optimal design of hybrid power systems', *Mathematics and Computers in Simulation*, Vol. 98, pp.46–62.

Akram, F., Asghar, F., Majeed, M.A., Amjad, W., Manzoor, M.O. and Munir, A. (2020) 'Techno-economic optimization analysis of stand-alone renewable energy system for remote areas', *Sustainable Energy Technologies and Assessments*, Vol. 38. Doi: 10.1016/j.seta.2020.100673.

Baghaee, H.R., Mirsalim, M. and Gharehpetian, G.B. (2017) 'Multi-objective optimal power management and sizing of a reliable wind/PV microgrid with hydrogen energy storage using MOPSO', *Journal of Intelligent and Fuzzy Systems*, Vol. 32, No. 3, pp.1753–1773.

Barakat, S., Ibrahim, H. and Elbaset, A.A. (2020) 'Multi-objective optimization of grid-connected PV-wind hybrid system considering reliability, cost, and environmental aspects', *Sustainable Cities and Society*, Vol. 60. Doi: 10.1016/j.scs.2020.102178.

Bhandari, B., Lee, K.T., Lee, G.Y., Cho, Y.M. and Ahn, S.H. (2015) 'Optimization of hybrid renewable energy power systems: A review', *International Journal of Precision Engineering and Manufacturing-Green Technology*, Vol. 2, No. 1, pp.99–112.

Chen, H., Li, W. and Yang, X. (2020) 'A whale optimization algorithm with chaos mechanism based on quasi-opposition for global optimization problems', *Expert Systems with Applications*, Vol. 158. Doi: 10.1016/j.eswa.2020.113612.

Das, M., Singh, M.A.K. and Biswas, A. (2019) 'Techno-economic optimization of an off-grid hybrid renewable energy system using metaheuristic optimization approaches–case of a radio transmitter station in India', *Energy Conversion and Management*, Vol. 185, pp.339–352.

Dhargupta, S., Ghosh, M., Mirjalili, S. and Sarkar, R. (2020) 'Selective opposition based grey wolf optimization', *Expert Systems with Applications*, Vol. 151. Doi: 10.1016/j.eswa.2020.113389.

El-Fergany, A.A. and Hasanien, H.M. (2015) 'Single and multi-objective optimal power flow using grey wolf optimizer and differential evolution algorithms', *Electric Power Components and Systems*, Vol. 43， No. 13, pp.1548–1559.

Eryilmaz, S., Bulanık, İ. and Devrim, Y. (2021) 'Reliability based modeling of hybrid solar/wind power system for long term performance assessment', *Reliability Engineering and System Safety*, Vol. 209. Doi: 10.1016/j.ress.2021.107478.

Gandomi, A.H. and Yang, X.S. (2014) 'Chaotic bat algorithm', *Journal of Computational Science*, Vol. 5, No. 2, pp.224–232.

Gupta, S. and Deep, K. (2020) 'A memory-based grey wolf optimizer for global optimization tasks', *Applied Soft Computing*, Vol. 93. Doi: 10.1016/j.asoc.2020.106367

Javed M.S., Song, A. and Ma, T. (2019) 'Techno-economic assessment of a stand-alone hybrid solar-wind-battery system for a remote island using genetic algorithm', *Energy*, Vol. 176, pp.704–717.

Jitkongchuen, D., Sukpongthai, W. and Thammano, A. (2017) 'Weighted distance grey wolf optimization with immigration operation for global optimization problems', *Proceedings of the 18th IEEE/ACIS International Conference on Software Engineering, Artificial Intelligence, Networking and Parallel/Distributed Computing (SNPD)*, IEEE, Japan, Kanazawa, pp.5–9.

Kamboj, V.K., Bath, S.K. and Dhillon, J.S. (2016) 'Solution of non-convex economic load dispatch problem using Grey Wolf Optimizer', *Neural Computing and Applications*, Vol. 27, No. 5, pp.1301–1316.

Komaki, G.M. and Kayvanfar, V. (2015) 'Grey Wolf Optimizer algorithm for the two-stage assembly flow shop scheduling problem with release time', *Journal of Computational Science*, Vol. 8, pp.109–120.

Liao, W.Q., Zhang, R.C., Wu, D.F., Yang, W.N. and Kai, Y. (2019) 'Multi-objective optimisation of ship microgrid research based on priority selective control strategy of diesel generator and energy storage', *International Journal of Computer Applications in Technology*, Vol. 59, No. 3, pp.193–204.

Liu, X., Tian, Y., Lei, X., Wang, H., Liu, Z. and Wang, J. (2019) 'An improved self-adaptive grey wolf optimizer for the daily optimal operation of cascade pumping stations', *Applied Soft Computing*, Vol. 75, pp.473–493.

Mirjalili, S., Mirjalili, S.M. and Lewis, A. (2014) 'Grey wolf optimizer', *Advances in Engineering Software*, Vol. 69, pp.46–61.

Mirjalili, S., Saremi, S., Mirjalili, S.M. and Coelho, L.D.S. (2016) 'Multi-objective grey wolf optimizer: a novel algorithm for multi-criterion optimization', *Expert Systems with Applications*, Vol. 47, pp.106–119.

Moradi, H., Esfahanian, M., Abtahi, A. and Zilouchian, A. (2018) 'Optimization and energy management of a standalone hybrid microgrid in the presence of battery storage system', *Energy*, Vol. 147, pp.226–238.

Pecora, L.M. and Carroll, T.L. (1990) 'Synchronization in chaotic systems', *Physical Review Letters*, Vol. 64, No. 8. Doi: 10.1103/PhysRevLett.64.821.

Saba, D., Laallam, F.Z., Belmili, H., Abanda, F.H. and Bouraiou, A. (2017) 'Development of an ontology-based generic optimisation tool for the design of hybrid energy systems', *International Journal of Computer Applications in Technology*, Vol. 55, No. 3, pp.232–243.

Salisu, S., Mustafa, M.W., Olatomiwa, L. and Mohammed. O.O. (2019) 'Assessment of technical and economic feasibility for a hybrid PV-wind-diesel-battery energy system in a remote community of north central Nigeria', *Alexandria Engineering Journal*, Vol. 58, No. 4, pp.1103–1118.

Sharafi, M. and Elmekkawy, T.Y. (2014) 'Multi-objective optimal design of hybrid renewable energy systems using PSO-simulation based approach', *Renewable Energy*, Vol. 68, pp.67–79.

Sulaiman, M.H., Mustaffa, Z., Mohamed, M.R. and Aliman, O. (2015) 'Using the gray wolf optimizer for solving optimal reactive power dispatch problem', *Applied Soft Computing*, Vol. 32, pp.286–292.

Sultan, H.M., Kuznetsov, O.N., Menesy, A.S. and Kamel, S. (2020) 'Optimal Configuration of a Grid-Connected Hybrid PV/Wind/Hydro-Pumped Storage Power System Based on a Novel Optimization Algorithm', *Proceedings of the International Youth Conference on Radio Electronics, Electrical and Power Engineering (REEPE)*, IEEE, Moscow, Russia, pp.1–7.

Wang, Y., Zhang, N., Chen, Q., Kirschen, D.S, Li, P. and Xia, Q. (2017) 'Data-driven probabilistic net load forecasting with high penetration of behind-the-meter PV', *IEEE Transactions on Power Systems*, Vol. 33, No. 3, pp.3255–3264.

Yahiaoui, A., Fodhil, F., Benmansour, K., Tadjine, M. and Cheggaga, N. (2017) 'Grey wolf optimizer for optimal design of hybrid renewable energy system PV-diesel generator-battery: application to the case of Djanet city of Algeria', *Solar Energy*, Vol. 158, pp.941–951.

Yang, D., Li, G. and Cheng, G. (2007) 'On the efficiency of chaos optimization algorithms for global optimization', *Chaos, Solitons and Fractals*, Vol. 34, No, 4, pp.1366–1375

Yang, H., Wei, Z. and Cheng, Z.L. (2009) 'Optimal design and techno-economic analysis of a hybrid solar–wind power generation system', *Applied Energy*, Vol. 86, No. 2, pp.163–169.

Zhang, D., Liu, J., Jiao, S., Tian, H., Lou, C., Zhou, Z. and Zuo, J. (2019a) 'Research on the configuration and operation effect of the hybrid solar-wind-battery power generation system based on NSGA-II', *Energy*, Vol. 189. Doi: 10.1016/j.energy.2019.116121.

Zhang, W., Maleki, A., Rosen, M.A. and Liu, J. (2019b) 'Sizing a stand-alone solar-wind-hydrogen energy system using weather forecasting and a hybrid search optimization algorithm', *Energy Conversion and Management*, Vol. 180, pp.609–621.